Wrong-Way Behavior of Packed-Bed Reactors: Influence of Interphase Transport

Large transient temperature excursions may be caused by a sudden reduction in the feed temperature to a packed-bed reactor operating at an intermediate conversion. When a unique steady state exists for all feed temperatures, the magnitude of the wrong-way behavior predicted by a two-phase model is very close to that predicted by a pseudohomogeneous model if Pe_H is equal to the dimensionless heat transfer coefficient H. The two-phase model enables a more efficient numerical simulation in such cases. The predictions of these two models may be rather different when steady-state multiplicity exists for some feed temperatures. In such cases, a two-phase model, which accounts for the axial dispersion of heat, should be used to simulate the transient behavior. The wrong-way behavior may lead to an ignition of a low-temperature state or an upstream propagation of a transient temperature wave.

Y. C. Chen
Dan Luss
Department of Chemical Engineering
University of Houston
Houston, TX 77204

Introduction

One of the most surprising dynamic features of a packed-bed reactor is the wrong-way behavior, under which a transient temperature increase is caused by a rapid reduction in the feed temperature. This temperature perturbation may shift the reactor to an undesired state or lead to a runaway. The wrong-way behavior is caused by the difference in the propagation speed of the concentration and temperature disturbances in the reactor. Thus, a sudden cooling of the feed reduces the conversion in the upstream section of the reactor. The increased reactant concentration causes a transient temperature rise in the downstream section of the reactor.

Boreskov et al. (1965), and Crider and Foss (1966) were the first to predict the occurrence of a wrong-way behavior in a packed-bed reactor. The wrong-way behavior was observed by Hoiberg et al. (1971) in a packed-bed reactor, in which a homogeneous liquid-phase reaction occurred; by Van Doesburg and De Jong (1976a, b) in the catalytic methanation of carbon monoxide; and by Sharma and Hughes (1979a, b) in the oxidation of carbon monoxide. The impact of the wrong-way behavior on the temperature excursion in an automobile convertor has been studied by Oh and Cavendish (1982).

Mehta et al. (1981) used a one-dimensional pseudohomogeneous plug-flow model to derive simple criteria predicting the conditions, under which the wrong-way behavior occurs, and its magnitude. That model ignored the axial dispersion of heat in the reactor as well as the transport resistances between the catalyst and fluid. Thus, it led to the prediction of a sharp temperature front (shock) with an unrealistically high peak temperature. Moreover, the model cannot predict an ignition of the reactor from a low-temperature steady state to a high-temperature steady state when multiple steady states exist, as observed experimentally by Sharma and Hughes (1979b).

Pinjala et al. (1988) found that the axial dispersion of heat decreases the magnitude of the temperature excursion, prolongs the transient shift to a new steady state, and may lead to some behavioral features that are qualitatively different from those predicted by the pseudohomogeneous plug-flow model. For example, the dispersion may create a temperature wave, which moves initially in the upstream direction. It may also ignite the reactor from a low-temperature state causing a disastrous runaway.

It is well known that the heat and mass transfer resistances between the fluid and catalyst may lead to steady-state multi-

Correspondence concerning this paper should be addressed to D. Luss.
Present address of Y. C. Chen: Air Products and Chemicals, Inc., PSG R&D-Iron Run, P.O. Box 2842, Lehigh Valley, PA 18001.

plicity in a packed-bed reactor even when no axial dispersion of heat exists (Liu and Amundson, 1963). The dispersion of any concentration or temperature perturbation by the interfacial transport resistances may be accounted for by an effective axial dispersion coefficient. However, these disturbances can propagate only in the downstream direction, in contrast to a diffusional mechanism under which disturbances can propagate in both upstream and downstream directions.

The goal of this work is to assess the impact of the interfacial and intraparticle heat and mass resistances on the wrong-way behavior. We start by comparing the predictions of a two-phase model, which accounts only for the interfacial transport resistances but ignores the axial dispersions of heat and mass, with those of a pseudohomogeneous model, which accounts for the axial dispersion of heat and mass. After determining the conditions under which both models predict a similar dispersion of heat, we compare their predictions of the wrong-way behavior. This enables us to determine the similarities and differences between the two models. Next, we examine a general model which accounts for both the interfacial transport resistances and axial dispersion. The results allow us to conclude which type of model should be used for an efficient prediction of the wrong-way behavior.

Development of the Mathematical Models

An adequate simulation of a packed-bed reactor may be obtained by a two-phase model, which accounts for the interfacial transport resistances between the particle and fluid, the intraparticle diffusional resistance, and the axial dispersion of heat and mass. The temperature gradient within a particle is usually small relative to the interfacial gradient (Carberry, 1975) and is ignored. The time constant for intraparticle concentration changes is usually much smaller than those of the pellet temperature, and the bulk concentration and temperature. Thus, we assume that the intraparticle concentration profile is in a pseudosteady state with respect to the pellet temperature and bulk conditions, so that the impact of the concentration gradient in the pellet can be accounted for by an isothermal effectiveness factor.

We assume that a single first-order irreversible reaction occurs in the reactor. The corresponding dimensionless species and energy balances are

$$\frac{1}{Le}\frac{\partial y}{\partial t} - \frac{1}{Pe_H}\frac{\partial^2 y}{\partial z^2} + \frac{\partial y}{\partial z} = H(y_s - y) + U(y_w - y) \quad (1)$$

$$\frac{1}{Le}\frac{\partial x}{\partial t} - \frac{1}{Pe_M}\frac{\partial^2 x}{\partial z^2} + \frac{\partial x}{\partial z} = M(x_s - x) \quad (2)$$

$$\left(1 - \frac{1}{Le}\right)\frac{\partial y_s}{\partial t} - H(y - y_s) = \beta\eta_s(y_s)\, x_s \exp\left[\frac{1}{y_r} - \frac{1}{y_s}\right] \quad (3)$$

$$M(x - x_s) = \eta_s(y_s)\, x_s \exp\left[\frac{1}{y_r} - \frac{1}{y_s}\right] \quad (4)$$

$$\eta_s(y_s) = \frac{3}{\phi_s^2}(\phi_s \coth \phi_s - 1) \quad (5)$$

where the dimensionless groups are defined as

$$x = C/C_f \qquad y = RT/E$$

$$Pe_M = \frac{Lu}{D_a} \qquad Pe_H = \frac{Lu\rho_f c_f}{\lambda_a}$$

$$Le = 1 + \frac{(1-\epsilon)\rho_s c_s}{\rho_f c_f \epsilon} \qquad t = \left(\frac{ut'}{\epsilon L}\right)\frac{1}{Le}$$

$$z = \frac{z'}{L} \qquad H = \frac{3hL(1-\epsilon)}{r_p u \rho_f c_f}$$

$$\beta = \frac{R}{E}\frac{(-\Delta H)C_f}{\rho_f c_f} \qquad M = \frac{3k_c L(1-\epsilon)}{r_p u}$$

$$U = \frac{2h_w L}{ru\rho_f c_f} \qquad \frac{k(y_r)}{k_o} = \exp(-1/y_r) = \frac{u}{Lk_o}$$

$$\phi_o^2 = \frac{r_p^2 k(y_r)}{D_e} = \frac{r_p^2 u}{D_e L}$$

$$\phi_s^2 = \phi_o^2 \exp\left(\frac{1}{y_r} - \frac{1}{y_s}\right) \quad (6)$$

The subscript, s, denotes the surface (pellet) value, and y_r is a reference temperature chosen so that $k(y_r) = u/L$. The corresponding boundary conditions are

$$y - y_f = \frac{1}{Pe_H}\frac{\partial y}{\partial z} \qquad z = 0 \quad (7)$$

$$1 - x = -\frac{1}{Pe_M}\frac{\partial x}{\partial z} \qquad z = 0 \quad (8)$$

$$\frac{\partial y}{\partial z} = \frac{\partial x}{\partial z} = 0 \qquad z = 1 \quad (9)$$

The initial conditions of all the state variables correspond to a steady state with a specified feed temperature y_{f1}. At $t = 0$, this feed temperature is suddenly reduced to a new value of y_{f2}.

It is of interest to compare the propagation of the transient temperature wave predicted by this general model for an adiabatic reactor with that by the single-phase model, which was analyzed by Pinjala et al. (1988). We assume that the transient temperature wave attains asymptotically a constant velocity, w, and assume that the intrinsic rate is $R(x_s, y_s)$. Introducing the new coordinate,

$$\mu = z - wt \quad (10)$$

and substituting the pseudosteady-state reaction rate determined by Eq. 4 into Eq. 2, the balance equations (Eqs. 1–4) can be transformed to

$$\frac{1}{Pe_H}\frac{d^2 y}{d\mu^2} - \left(1 - \frac{w}{Le}\right)\frac{dy}{d\mu} = H(y - y_s) \quad (11)$$

$$\frac{1}{Pe_M}\frac{d^2 x}{d\mu^2} - \left(1 - \frac{w}{Le}\right)\frac{dx}{d\mu} = \eta_s(x_s, y_s)R(x_s, y_s) \quad (12)$$

$$\left(1 - \frac{1}{Le}\right)w\frac{dy_s}{d\mu} = H(y_s - y) - \beta\eta_s(x_s, y_s)R(x_s, y_s) \quad (13)$$

Adding Eqs. 11, 13 and β multiplied by Eq. 12 gives

$$\frac{\beta}{Pe_M}\frac{d^2x}{d\mu^2}+\frac{1}{Pe_H}\frac{d^2y}{d\mu^2}-\beta\left(1-\frac{w}{Le}\right)\frac{dx}{d\mu}-\left(1-\frac{w}{Le}\right)\frac{dy}{d\mu}+\left(1-\frac{1}{Le}\right)w\frac{dy_s}{d\mu}=0 \quad (14)$$

Equation 11 can be used to determine y_s in terms of y and its derivatives. Using that expression, Eq. 14 becomes

$$-\frac{w\left(1-\frac{1}{Le}\right)}{Pe_H H}\frac{d^3y}{d\mu^3}+\left[\frac{1}{Pe_H}+\left(1-\frac{1}{Le}\right)\frac{w}{H}\left(1-\frac{w}{Le}\right)\right]\frac{d^2y}{d\mu^2}+\frac{\beta}{Pe_M}\frac{d^2x}{d\mu^2}+(w-1)\frac{dy}{d\mu}-\beta\left(1-\frac{w}{Le}\right)\frac{dx}{d\mu}=0 \quad (15)$$

In practice, Pe_M, Pe_H, H, and Le are all much larger than unity, w is of order one, and order of magnitude arguments can be used to approximate Eq. 15 by

$$\frac{w}{Pe_{H^*}}\frac{d^2y}{d\mu^2}+\frac{\beta}{Pe_M}\frac{d^2x}{d\mu^2}+(w-1)\frac{dy}{d\mu}-\beta\frac{dx}{d\mu}=0 \quad (16)$$

where

$$\frac{w}{Pe_{H^*}}=\frac{1}{Pe_H}+\frac{w}{H}$$

For a temperature wave propagating at a unit speed ($w = 1$), we obtain

$$\frac{1}{Pe_{H^*}}=\frac{1}{Pe_H}+\frac{1}{H} \quad (17)$$

It is of interest to note that this result is independent of the intrinsic rate expression $R(x_s, y_s)$. Comparing Eq. 16 with the derivations by Pinjala et al. (1988), we conclude that the asymptotic dispersion of the temperature wave described by the general model can be approximated by the pseudohomogeneous model with a modified Peclet number defined by Eq. 17. Moreover, it suggests that the predictions of the two-phase plug-flow model ($Pe_H \to \infty$) should be very close to those of the pseudohomogeneous axial dispersion model ($H \to \infty$), if we select

$$Pe_H \approx H \quad (18)$$

and w close to unity. In practice, H and Pe_H are finite, and the pseudohomogeneous model with the modified Peclet number and the two-phase model with the modified H, should predict the same behavior if one chooses $H = Pe_{H^*}$. We do not expect the relation defined by Eq. 18 to be adequate when w is much smaller than unity. The predictions of these two models are definitely different when w is negative, i.e., when the axial dispersion model causes a backward (upstream) movement of the temperature wave.

It is well known that the interfacial and/or intraparticle heat and mass resistances, as well as the axial dispersion of heat, may lead to the existence of multiple steady states in a packed-bed reactor, i.e., different steady states may exist under the same operating conditions. We shall study separately the impact of the wrong-way behavior under the conditions for which a unique or multiple steady states exist. We shall examine first the behavior of a limiting model, in which we ignore the axial dispersion of heat and mass and assume that the intraparticle diffusional resistance is negligible ($Pe_H \to \infty$ and $\phi_o = 0$). We shall later check the impact of the intraparticle diffusional limitation on the reactor behavior. We shall then check the predictions and insight gained from the simplified limiting models with those obtained from the general model.

In all the simulations reported in this work, unless otherwise indicated, we assumed for the two-phase model that $M = 540$ and $H = 180$, and for the axial dispersion model that $Pe_H = 180$ and $Pe_M = 720$. The reactor is assumed to be adiabatic and with negligible diffusion limitations, i.e., $U = 0$ and $\phi_o = 0$, unless otherwise specified. The pseudohomogeneous model was solved numerically by a finite difference method with an adjustable grid size in t and z. The two-phase model was solved using the characteristics method (Aris and Amundson, 1973).

Analysis of Wrong-Way Behavior

We study first the wrong-way behavior using a limiting two-phase model assuming that the axial dispersion of heat and mass is negligible. In this case, Eqs. 1–4 reduce to a set of first-order differential equations, which can be solved by the method of characteristics (Aris and Amundson, 1973).

We consider first the case in which the reactor has a unique steady-state solution for all feed temperatures, so that the maximal steady-state temperature in the reactor, y_{max}, is a unique, monotonically increasing function of the feed temperature, y_f (Figure 1). Four different types of steady-state behavior exist depending on the feed temperature. At a sufficiently low-feed temperature ($y_f \ll y_r$), denoted as Region a in Figure 1, a low

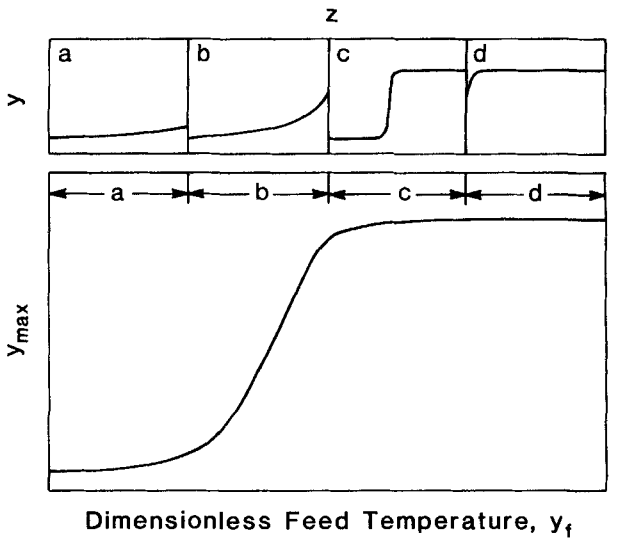

Figure 1. Division of the dimensionless feed temperature into four regions with different steady-state behavior (shown in insets) for a case that a unique solution exists for all feed temperatures.

conversion and a small temperature rise occur in the reactor. Region *b* consists of feed temperatures for which an intermediate level of conversion occurs in the reactor. Region *c* consists of feed temperatures for which essentially a complete conversion occurs, with a sharp reaction zone within the reactor. Finally, Region *d* consists of high feed temperatures for which a very high conversion occurs in a narrow zone close to the reactor inlet. A schematic diagram of the steady-state temperature profile in each region is shown in Figure 1.

The numerical simulation shows that the wrong-way behavior predicted by the heterogeneous plug-flow model is very similar to that predicted by the pseudohomogeneous axial-dispersion model used by Pinjala et al. (1988) assuming $Pe_H = H$. For each model, the qualitative features of the wrong-way behavior are rather different in each of the four regions of feed temperatures (Figure 1). In region *a*, a sudden decrease in the feed temperature causes a negligible transient temperature rise. The temperature wave moves out of the reactor with a unit dimensionless speed. For a reactor operating in Region *b*, a sudden reduction in the feed temperature leads to a transient temperature increase in the downstream section of the reactor. The transient temperature wave moves out of the reactor also at a unit speed.

A sudden decrease in the feed temperature for a reactor operating in Region *c* reduces the upstream temperature to that of the new steady state rapidly (Figure 2). This increases the upstream reactant concentration leading to a sharp temperature rise in a narrow zone in which the reactant is consumed. The temperature profile eventually attains a constant shape and moves downstream with a dimensionless speed smaller than unity. The simulation shows that, as the step change in the feed temperature is increased, the transient peak temperature approaches an asymptotic value of y^*, which is the maximum transient temperature attainable in Regions *b* and *c*. It was shown by Pinjala et al. (1988) that y^* is also the boundary between regions *c* and *d* in the steady-state diagram (Figure 1). The peak temperature, y^*, is obtained, when the new feed temperature, y_{f2}, is rather low. A reduction in the feed temperature in Region *d* leads to a very small transient temperature increase.

Figure 3 is a master diagram describing the dependence of the maximal transient temperature (dashed lines) on the initial (solid line) and new feed temperatures for four initial feed temperatures, each in a different operating region. The solid line in the diagram gives the maximal steady-state temperature at the corresponding feed temperature. Each dashed line describes the dependence of the maximal transient temperature on the feed temperature for an initial feed temperature represented by the intersection of the dashed and solid lines. The calculations were conducted for a fixed H value of 180 and a wide range of M values (54 to 5,400). The change in the value of M has a negligible impact on the transient temperature rise in regions *a* and *d*. However, it has some impact in regions *b* and *c*. The dashed areas in Figure 3 represent the range of values obtained. Increasing M increases the maximal transient temperature. The

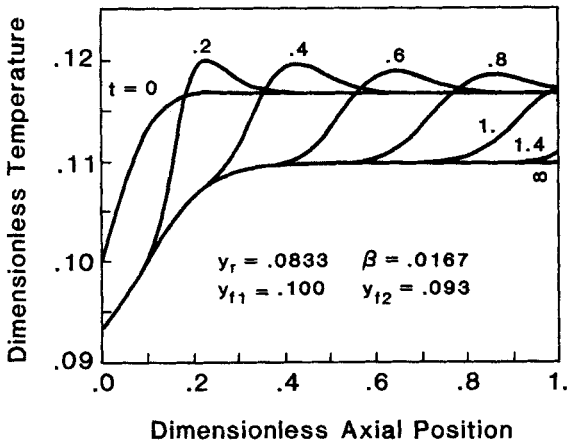

Figure 2. Typical response to a sudden feed temperature decrease in Region c.

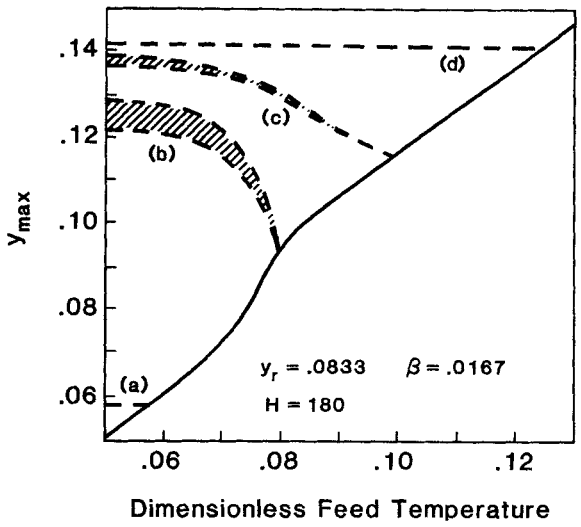

Figure 3. Dependence of the maximal transient temperature (dashed lines) on the original (solid line) and the new feed temperature for *M* values in the range of 54 to 5,400.

Letters refer to regions in which original steady state was.

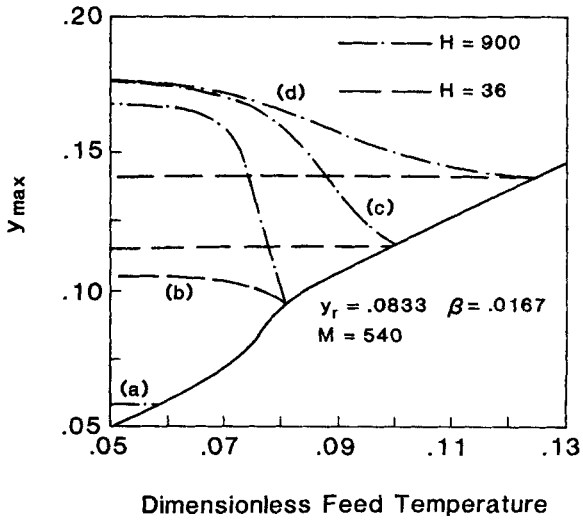

Figure 4. Dependence of the maximal transient temperature on the original (solid line) and the new feed temperature for H = 900 (dash-dot line) and H = 36 (dashed line).

Letters refer to regions in which original state was.

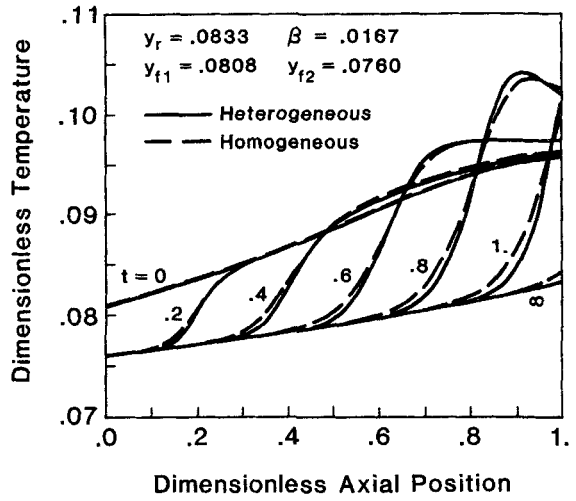

Figure 5. Typical response to a feed temperature decrease in Region *b*.

largest transient temperature increase is obtained when the reactor operates in Region *b*.

Figure 4 is a master diagram similar to Figure 3, which shows the impact of changing H from 36 to 900 for a fixed M value of 540. The calculations show that, unlike the changes in M, the changes in the value of H can have a rather strong impact on the maximal transient temperature, especially for operation in Regions *b* and *c*. Increasing the value of H tends to increase the maximal transient temperature.

The simulations show that the predicted transient behavior of the two-phase model is very close to that of the dispersion model with $Pe_H = H$, in agreement with Eq. 18. A comparison of the transient behavior for a typical case in Region *b* is shown in Figure 5, which indicates that the two models predict essentially the same behavior. Accounting for the intraparticle diffusion does not affect this similarity.

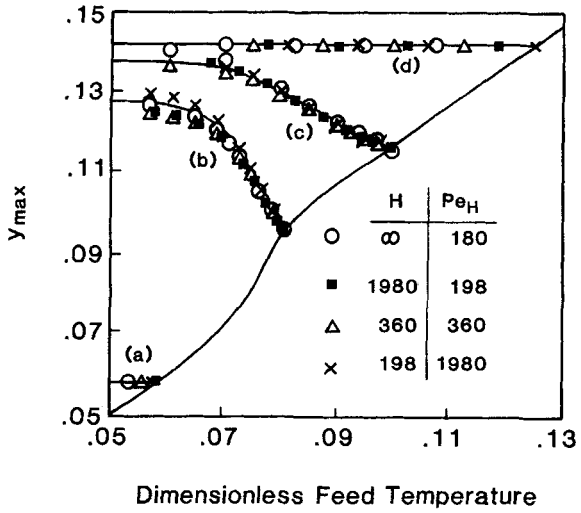

Figure 6. Dependence of the maximal transient temperature on the original and new feed temperatures for four cases and three models when y_f = 0.0833 and β = 0.0167.

The two-phase model is shown by a solid line, the pseudohomogeneous model by open circles. The other three cases are of the general model. In all the cases, $M = 3H$ and $Pe_M = 4Pe_H$.

Figure 6 is a master diagram, which compares the maximum transient temperatures at different feed temperatures, as computed by the two limiting models and the general model. In accordance with Eq. 18, the predictions of the two-phase model (solid line) agree very well with those of the pseudohomogeneous axial dispersion model (open circles) when a unique steady state exists for all feed temperatures. The comparison with the general model prediction will be done later. This close similarity suggests that one should use the two-phase model, as its numerical simulation is much simpler and requires less CPU time. (The exact gain in CPU time depends on the operating conditions.)

The behavior of the reactor is more intricate when two stable steady-state solutions exist at some feed temperatures. The analysis using the axial-dispersion model was presented by Pinjala et al. (1988). When the two-phase model with no axial dispersion is used, the steady-state diagram of y_{max} vs. y_f consists of two stable branches. The upper one, which we shall call the high-temperature branch (shown as a solid line in Figure 7), consists of all the states in which each particle is at the high-temperature state if it can attain different steady states. Similarly, the low-temperature branch consists of all the states in which each particle is at the low-temperature steady state when multiplicity exists for the particle. The low-temperature branch is shown by the dash-dot line in Figure 7 as well as the solid line (U_1, U_2). For all feed temperatures in section (U_1, U_2), the exit temperature of the high-temperature branch is equal to that of the low-temperature branch. Thus, in this range of feed temperatures, there exist multiple steady states with different temperature and concentration profiles, but with the same maximal temperature. For a feed temperature higher than U_2, a unique steady state exists.

The simulations show that the behavior on each branch is rather similar to that observed in the case of a unique steady state (Figure 3). Thus, the behavior in each branch can be divided into four regions. Figure 7 shows the maximal transient

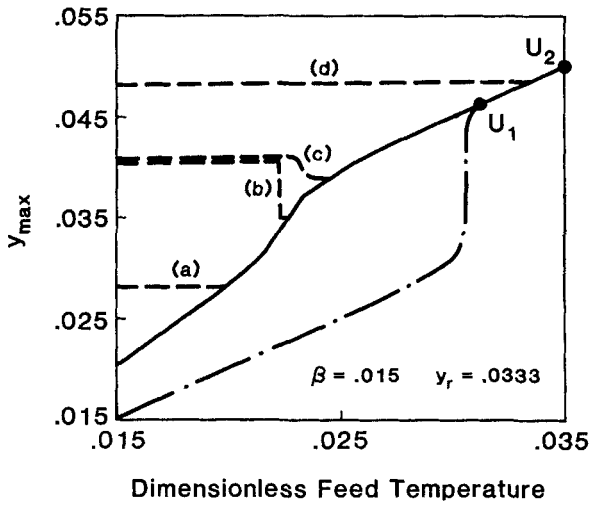

Figure 7. Maximal transient temperature vs. feed temperature as predicted by the two-phase model in the four regions of the high-temperature branch, shown by solid line.

temperature vs. the feed temperature in the four regions of the high-temperature branch. The results show that a negligible transient temperature rise occurs in Regions *a* (low conversion) and *d* (very high conversion), while a rather large temperature rise is reached in Regions *b* and *c*. The maximal transient temperature in Regions *b* and *c* reaches an asymptotic value for a large feed temperature decrease.

The response of the reactor, operating in Region *b* of the high-temperature branch, to a rapid feed temperature decrease is described in Figure 8. The simulation shows that a temperature wave is formed at the downstream section of the reactor, which moves through the reactor at a speed smaller than unity.

The transient response from an initial steady state on the low-temperature branch to a feed temperature decrease is also similar to that when a unique solution exists. Again, the response can be classified into four regions (Figure 9). A negligible temperature rise is found in Regions *a* and *d*. The largest and most drastic temperature rise occurs for states with an intermediate value of conversion (Region *b*), where the slope of the steady-state solution is very sensitive to a change in the feed temperature. Comparing the behavior of the high- and low-temperature branches (Figures 7 and 9), we note that, while the behavior of each branch is qualitatively similar to that of a unique steady state (Figure 6), the transient temperature rise on each branch depends mainly on the initial conversion and not the feed temperature. Thus, the same initial feed temperature may belong to a different region of the two branches. For example, for an initial feed temperature of 0.025, the high-temperature state is in Region *c* (Figure 7), while the low-temperature state is in Region *a* (Figure 9). We also note that the low-temperature branch has a rather sharp increase in its slope in a very narrow range of feed temperatures. No similar sensitivity to a small change in the feed temperature is observed on the high-temperature branch. This is the main reason that a much larger transient temperature rise is observed in Region *b* of the low-temperature branch.

Our study shows that the range of feed temperatures, over which steady-state multiplicity occurs, is much larger for the

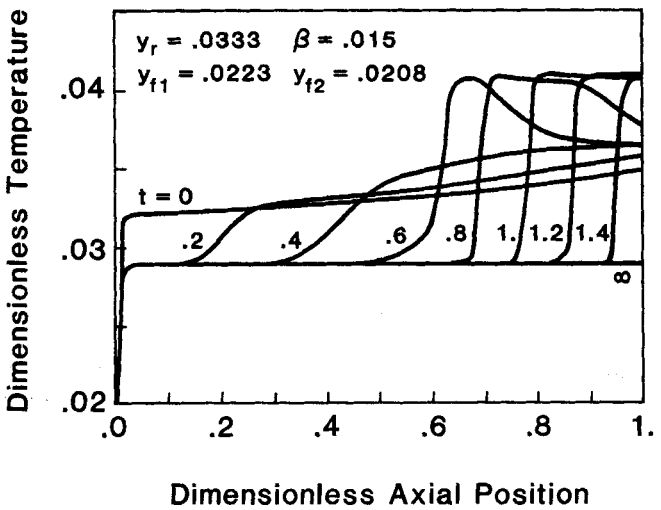

Figure 8. Typical response of a reactor operating in Region *b* of the high-temperature branch to a sudden feed temperature decrease.

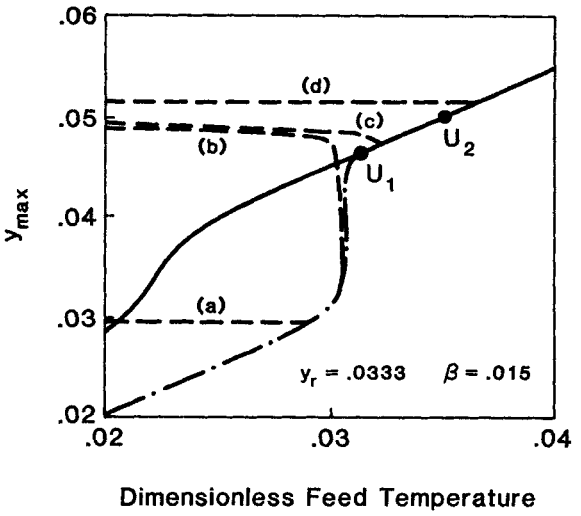

Figure 9. Maximal transient temperature vs. feed temperature in the four regions of the low-temperature branch, shown by dash-dot line and solid section U_1, U_2.

two-phase model than for the pseudohomogeneous axial dispersion model. In the example shown in Figure 7, multiplicity exists for all feed temperatures in (0.0052, 0.0349) for the two-phase model, while multiplicity exists only for a much smaller range of y_f (0.0295, 0.0306) for the axial dispersion model with $Pe_H = H$. The two-phase model, however, is not capable of predicting a thermal wave propagating in the upstream direction, a behavior which was observed and can be predicted by a model accounting for the axial dispersion. Thus, an ignition from the low-temperature steady state to the high-temperature steady state which is accompanied by an upstream heating requires the use of a model accounting for the axial dispersion. It is important to remember this potential pitfall of the two-phase model when the reactor can attain multiple steady states.

Intraparticle diffusion tends to decrease the range of feed temperatures over which multiplicity exists in the two-phase model and, in some cases, may even eliminate the multiplicity. In the examples shown in Figures 7 and 9, intraparticle diffusion is ignored and multiplicity is predicted over a wide range of feed temperatures. If one assumes that a diffusional limitation exists with $\phi_o = 10$, a unique solution is obtained for all feed temperatures (Figure 10). The diffusion limitation shifts the y_{max} vs. y_f curve to the right of the low-temperature branch predicted for $\phi_o = 0$. The diffusional limitation may lead to a higher transient temperature rise than in its absence. For example, Figure 11a describes the wrong-way behavior for a reactor operating in Region *d* and with a negligible diffusion limitation. Accounting for the diffusion limitation shifts the reactor to Region *c*, which leads to a much larger temperature excursion with the same reduction in the feed temperature (Figure 11b).

The complete model (Eqs. 1–4), which accounts for the transport resistances between the two phases as well as the axial dispersion of heat and mass, predicts all the features described by any of the limiting models. Figure 6 shows that, when a unique steady state exists, the maximal transient temperature rise predicted by the complete model is very close to that predicted by either one of the two limiting models, if one uses either a Pe_H

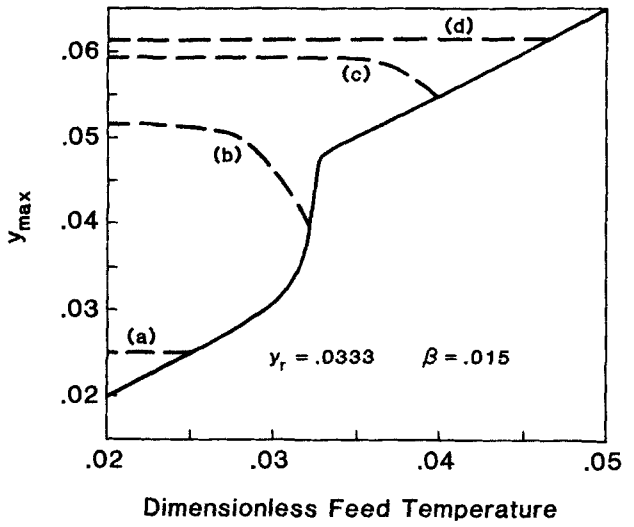

Figure 10. Maximal transient temperature vs. feed temperature for a case with intraparticle diffusional limitation (Φ_o = 10).

equal to Pe_{H^*} (as predicted by Eq. 17) in the pseudohomogeneous model or sets $H = Pe_{H^*}$ in the two-phase model. The main advantage of the general model is that it does not have any of the pitfalls that the limiting models have in the region of steady-state multiplicity. Specifically, the general model predicts correctly a much larger region of multiplicity than does the pseudohomogeneous model; unlike the two-phase model, it is capable of predicting a backward propagation of thermal waves and subsequent ignition. Figures 12–13 illustrate such a case, in which the following parameter values were assumed: H = 1,125, Pe_H = 25, M = 4,500, Pe_M = 100, β = 0.0708, Le = 500, U = 1, and ϕ_o^2 = 15. Pinjala et al. (1988) have shown that, when multiple steady states exist, there are five regions with different wrong-way behavior may exist. In this case, the reactor is initially in Region c, and the sudden cooling leads to ignition. The two figures describe the propagation of the temperature waves in the solid and gas phases, respectively. The strong cooling of the reactor leads to the formation of a sharp temperature peak in the solid phase. The gas temperature profiles are much smoother than the solid temperature profiles.

The simulations of the complete model require significantly more computer time than either one of the two limiting models. We recommend that it be used when multiple steady states exist. On the other hand, when a unique steady state exists, the predictions of the two-phase model are usually very close to those of the general model, but are obtained at a reduced computational effort.

Conclusions and Remarks

This work confirms the predictions of Pinjala et al. (1988) that a sudden feed temperature reduction leads to a negligible temperature excursion when the conversion in the reactor is very low or very high, but can lead to an appreciable temperature excursion for a reactor with an intermediate level of conversion.

In most applications, a packed-bed reactor has a unique steady state for all feed temperatures. In such cases, both the two-phase model and the pseudohomogeneous axial dispersion

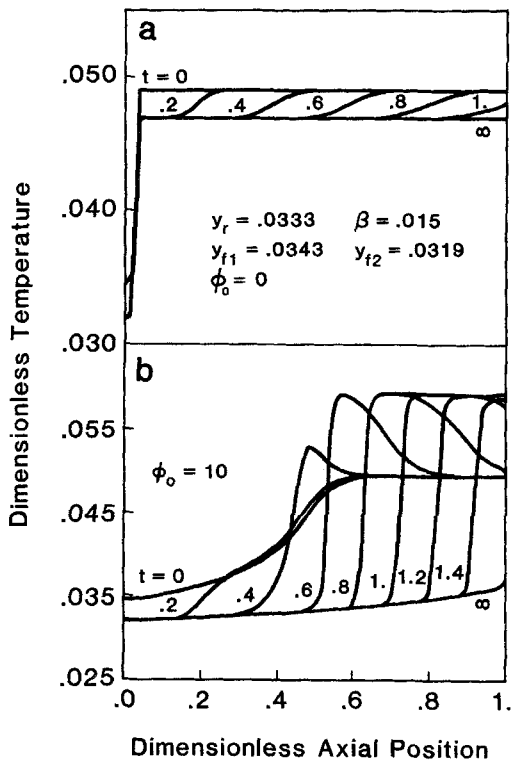

Figure 11. Typical response of a reactor to a sudden temperature decrease.
In Case a, Φ_o = 0 so that the reactor is in Region d. In Case b, Φ_o = 10 and the reactor is in Region c.

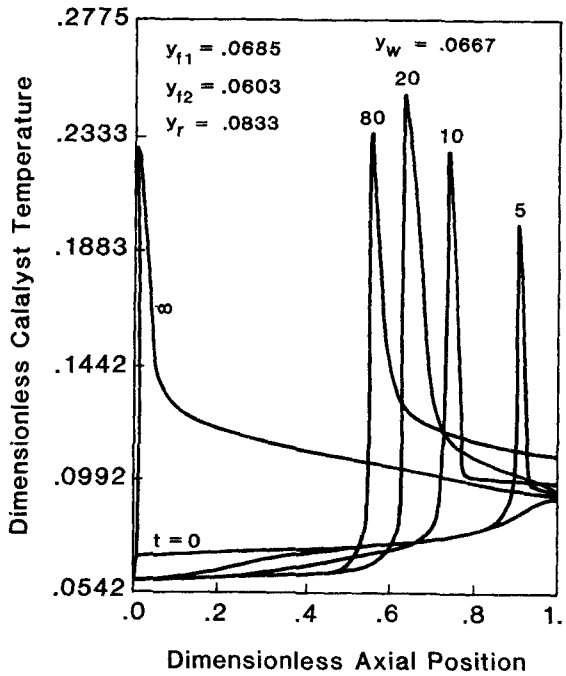

Figure 12. Transient solid temperature profiles following a sudden feed temperature decrease.
Predicted by a heterogeneous model accounting for the axial dispersion and intraparticle diffusional limitation.

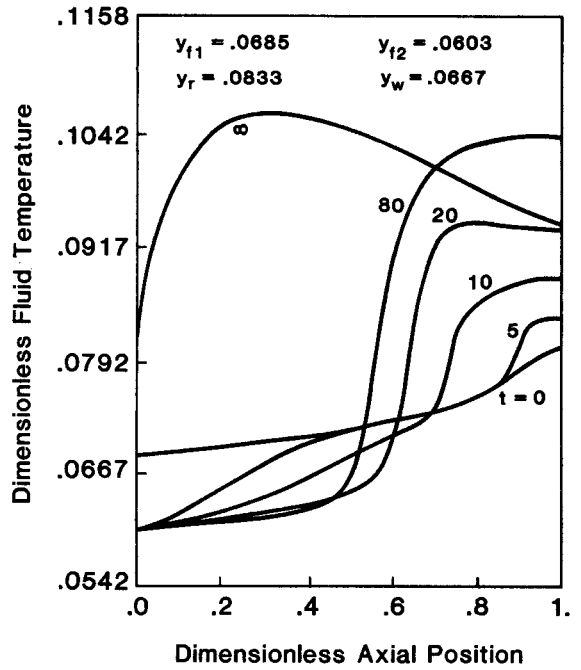

Figure 13. Transient gas temperature profiles corresponding to the case shown in Figure 12.

model predict essentially the same magnitude of transient temperature excursion when we select $Pe_H = H$. When a unique steady state exists, the predictions of the general model are equal to those of either limiting model if one uses the relation defined by Eq. 17. The two-phase model is computationally more efficient than a model accounting for the axial dispersion. Thus, we recommend its use in these cases.

A large deviation between the predictions of the various models may occur when steady-state multiplicity exists for some feed temperatures. The region of multiplicity predicted by the two-phase model is much larger than that predicted by the pseudohomogeneous model with $Pe_H = H$. This occurs because the source of multiplicity in the two-phase model is the interfacial transport resistances, which can readily lead to multiplicity for a typical set of parameters. In the pseudohomogeneous model, the multiplicity is induced by the axial backmixing of heat, which is less likely to lead to multiplicity under typical operating conditions. The main disadvantage of the two-phase model is that it cannot predict the backward migration of the temperature wave and subsequent ignition, a behavior which is sometimes observed. Thus, we recommend that if the reactor operates at an intermediate level of conversion in the region of multiplicity, one should use the complete model, which accounts for both the axial dispersion of heat and the interfacial resistances.

Acknowledgments

The authors wish to acknowledge the donors of the Petroleum Research Fund administered by the American Chemical Society and the National Science Foundation for the support of this study.

Notation

C = concentration of reactant
c = specific heat
D_a = axial mass dispersion coefficient
D_e = effective diffusivity
E = activation energy
H = dimensionless interfacial heat transfer parameter, defined by Eq. 6
$(-\Delta H)$ = heat of reaction
h = interfacial heat transfer coefficient
h_w = overall heat transfer coefficient at wall
k_c = interfacial mass transfer coefficient
k_o = pre-exponential factor
L = reactor length
Le = Lewis number, defined by Eq. 6
M = dimensionless mass transfer parameter, defined by Eq. 6
Pe_H = Peclet number for heat, defined by Eq. 6
Pe_{H^*} = modified Peclet number for heat, defined by Eq. 17
Pe_M = Peclet number for mass, defined by Eq. 6
R = universal gas constant
r = reactor radius
r_p = particle radius
$R(x_s, y_s)$ = intrinsic rate expression
T = temperature
t = dimensionless time, defined by Eq. 6
t' = time
U = dimensionless heat transfer parameter, defined by Eq. 6
u = superficial velocity
w = dimensionless propagation speed of temperature wave
x = dimensionless concentration, C/C_f
y = dimensionless temperature, RT/E
y_r = dimensionless characteristic temperature, defined by Eq. 6
y^* = maximal transient peak temperature
z' = axial position coordinate
z = dimensionless axial position, z'/L

Greek letters

β = dimensionless adiabatic temperature rise, defined by Eq. 6
ϵ = void fraction of bed
ϕ_o = Thiele modulus at $y = y_r$, defined by Eq. 6
ϕ_s = Thiele modulus at $y = y_s$, defined by Eq. 6
η_s = isothermal effectiveness factor, defined by Eq. 5
λ_a = axial heat dispersion coefficient
μ = dimensionless axial position, $z - wt$
ρ = density

Subscripts

1 = initial steady state
2 = new steady state
f = feed, fluid
s = solid
w = wall

Literature Cited

Aris, R., and N. R. Amundson, *Mathematical Methods in Chemical Engineering: 2. First-Order Partial Differential Equations with Applications*, Prentice-Hall, Englewood Cliffs, NJ (1973).

Boreskov, G. K., and M. G. Slinko, "Modelling of Chemical Reactors," *Pure Appl. Chem.*, **10**, 611 (1965).

Carberry, J., "On the Relative Importance of External-Internal Temperature Gradients in Heterogeneous Catalysts," *Ind. Eng. Chem. Fund.*, **14**, 129 (1975).

Crider, J. E., and A. S. Foss, "Computational Studies of Transients in Packed Tubular Chemical Reactors," *AIChE J.*, **12**, 514 (1966).

Hoiberg, J. A., B. C. Lyche, and A. S. Foss, "Experimental Evaluation of Dynamic Models for a Fixed-Bed Catalytic Reactor," *AIChE J.*, **17**, 1434 (1971).

Liu, S. L., and N. R. Amundson, "Stability of Nonadiabatic Packed-Bed Reactor," *Ind. Eng. Chem. Fund.*, **2**, 12 (1963).

Mehta, P. S., W. N. Sams, and D. Luss, "Wrong-Way Behavior of Packed-Bed Reactors: I. The Pseudo-Homogeneous Model," *AIChE J.*, **27**, 234 (1981).

Oh, S. H., and J. C. Cavendish, "Transients of Monolithic Catalytic Convertors: Response to Step Changes in Feedstream Temperature as

Related to Controlling Automobile Emissions," *I.E.C. Proc. Des. Dev.*, **21**, 29 (1982).

Pinjala, V., Y. C. Chen, and D. Luss, "Wrong-Way Behavior of Packed-Bed Reactors: II. Impact of Thermal Diffusion," *AIChE J.*, **34**, 1663 (1988).

Sharma, C. S., and R. Hughes, "The Behavior of an Adiabatic Fixed Bed Reactor for the Oxidation of Carbon Monoxide: I. General Parametric Studies," *Chem. Eng. Sci.*, **34**, 613 (1979a).

Sharma, C. S., and R. Hughes, "The Behavior of an Adiabotic Fixed Bed Reactor for the Oxidation of Carbon Monoxide: II. Effect of Perturbations," *Chem. Eng. Sci.*, **34**, 625 (1979b).

Van Doesburg, H., and W. A. De Jong, "Transient Behavior of an Adiabatic Fixed-Bed Methanator: I. Experiments with Binary Feeds of CO or CO_2 in Hydrogen," *Chem. Eng. Sci.*, **31**, 45 (1976a).

Van Doesburg, H., and W. A. De Jong, "Transient Behavior of an Adiabatic Fixed-Bed Methanator: II. Methanation of Mixtures of Carbon Monoxide and Carbon Dioxide," *Chem. Eng. Sci.*, **31**, 53 (1976b).

Manuscript received Jan. 17, 1989, and revision received May 8, 1989.